

Strongly Lensed Gravitational Waves and Electromagnetic Signals as Powerful Cosmic Rulers

Jun-Jie Wei^{1,2*} and Xue-Feng Wu^{1,3,4†}

¹*Purple Mountain Observatory, Chinese Academy of Sciences, Nanjing 210008, China*

²*Guangxi Key Laboratory for Relativistic Astrophysics, Nanning 530004, China*

³*School of Astronomy and Space Sciences, University of Science and Technology of China, Hefei 230026, China*

⁴*Joint Center for Particle, Nuclear Physics and Cosmology, Nanjing University-Purple Mountain Observatory, Nanjing 210008, China*

Accepted XXX. Received YYY; in original form ZZZ

ABSTRACT

In this work, we discuss the possibility of using strongly lensed gravitational waves (GWs) and their electromagnetic (EM) counterparts as powerful cosmic rulers. In the EM domain, it has been suggested that the joint observations of the time delay ($\Delta\tau$) between lensed quasar images and the velocity dispersion (σ) of the lensing galaxy (i.e., the combination $\Delta\tau/\sigma^2$) have a stronger constraint ability on the cosmological parameters than $\Delta\tau$ or σ^2 separately. Here we first propose that this $\Delta\tau/\sigma^2$ method can be applied to the strongly lensed systems observed in both GW and EM windows. Combining the redshifts, images, and σ observed in the EM domain with the very precise $\Delta\tau$ derived from lensed GW signals, we expect that accurate multi-messenger cosmology can be achieved in the era of third-generation gravitational-wave detectors. Comparing with the constraints from the $\Delta\tau$ method, we prove that using $\Delta\tau/\sigma^2$ can improve the discrimination between cosmological models. Furthermore, we demonstrate that with several tens of strongly lensed GW-EM systems, one may reach a constraint on the dark energy equation of state w comparable to the 580 Union2.1 Type Ia supernovae data. Much more stringent constraints on w may be obtained when combining the $\Delta\tau$ and $\Delta\tau/\sigma^2$ methods.

Key words: gravitational lensing; strong – gravitational waves – cosmological parameters – dark energy – distance scale

1 INTRODUCTION

In the standard Λ CDM cosmological model, it is currently inferred that $\sim 96\%$ of the total energy density of the Universe is consist of dark matter ($\sim 26\%$) and dark energy ($\sim 70\%$). These proportions have been measured precisely via various standard candles or rulers, such as Type Ia supernovae (SNe Ia; [Perlmutter et al. 1998](#); [Riess et al. 1998](#); [Schmidt et al. 1998](#); [Suzuki et al. 2012](#)), anisotropy of the cosmic microwave background (CMB) radiation ([Hinshaw et al. 2013](#); [Planck Collaboration et al. 2016](#)), as well as baryon acoustic oscillations ([Beutler et al. 2011](#); [Anderson et al. 2012](#)). Though cosmology has entered a new era of precision tests, we should note that all of the cosmological probes are based on electromagnetic (EM) observations alone. In 1986, [Schutz \(1986\)](#) first proposed that the waveform signal of gravitational wave (GW) from inspiraling and merging compact binaries encodes the luminosity

distance d_L information, proving an access to the direct measurement of d_L . Thus the GW signals can be considered as standard sirens. The combination of d_L derived from GWs and redshifts z derived from their EM counterparts would make the GW events an ideal tool to constrain the cosmological parameters and the equation of state of dark energy.

On February 11, 2016, the Laser Interferometer Gravitational Wave Observatory (LIGO) team reported the first direct detection of the gravitational wave source (GW 150914; [Abbott et al. 2016a](#)), opening a brand new window for studying the Universe, which indicates that the era of multi-messenger cosmology is coming. In the past, several studies have investigated the possibility of GWs as standard sirens (e.g., [Holz & Hughes 2005](#); [Cai & Yang 2017](#); [Del Pozzo et al. 2017](#)). Particularly, [Cai & Yang \(2017\)](#) found that with about 500–600 simulated GW events they can determine the Hubble constant H_0 with an accuracy comparable to Planck 2015 results; while for the dark matter density parameter Ω_m , it should need more than 1000 GW events to match the Planck sensitivity.

Very recently, [Fan et al. \(2017\)](#) presented a new model-

* E-mail: jjwei@pmo.ac.cn (JJW)

† E-mail: xfwu@pmo.ac.cn (XFW)

independent method for constraining the speed of GWs, based on future time delay measurements of strongly lensed GWs and their EM counterparts (see also Baker & Trodden 2017; Collett & Bacon 2017). Even more encouragingly, Liao et al. (2017) proved that such strongly lensed GW-EM systems could also provide strong constraints on cosmological parameters. The GW standard-sirens method in cosmology appeals to the luminosity distance measurement from the GW observation which relies on the fine details of the waveform, but the proposed method of Liao et al. (2017) is waveform independent. Moreover, the GW standard-sirens method would require several hundreds of GW events to match the Planck sensitivity on H_0 (i.e., with $\sim 1.3\%$ uncertainty; Cai & Yang 2017), while Liao et al. (2017) showed that the uncertainty of H_0 can be limited to $\sim 0.2\%$ only with dozens of lensed GW-EM events. That is, combining the redshifts and images observed in the EM domain with the high-accuracy time delay measurements from lensed GW signals, one may achieve precise cosmography. Note that the time delays between different lensed images ($\sim 10 - 100$ days) obtained from the GW observations would reach an unprecedented accuracy of ~ 0.1 s from the detection pipeline. Compared to the uncertainty in lens modeling, the uncertainty of the GW time delay is negligible.

In the EM window, strongly gravitationally lensed quasar-galaxy systems have been deemed as a complementary cosmological probe (see, e.g., Refsdal 1964; Treu 2010). The Einstein ring radius inferred from the deflection angle and the time delay between different lensed images can provide the information of angular-size distance independently, which can be used to measure cosmological parameters (see, e.g., Zhu 2000; Grillo et al. 2008; Coe & Moustakas 2009; Dobke et al. 2009; Paraficz & Hjorth 2009, 2010; Biesiada et al. 2010; Cao et al. 2012; Suyu et al. 2013; Sereno & Paraficz 2014; Bonvin et al. 2017) and discriminate different cosmological models (see, e.g., Zhu & Sereno 2008; Wei et al. 2014; Melia et al. 2015; Yuan & Wang 2015). As of today, the observation of about 70 strong gravitational lensing systems and 12 two-images lensing systems with time delay measurements has provided the data that, in principle, can be used to carry out the study of cosmology. But this is only the beginning. The upcoming Large Synoptic Survey Telescope (LSST) will find more than ~ 8000 lensed quasars, about 3000 of which will have well-measured time delays within ten years (Oguri & Marshall 2010). The number of robust time-delay measurements for probing cosmology is estimated to be ~ 400 , each with precision $< 3\%$ and accuracy of $\sim 1\%$ (Dobler et al. 2015; Liao et al. 2015). In addition, we note that an interesting cosmic ruler constructed from the joint measurements of the time delay ($\Delta\tau$) between lensed quasar images and the velocity dispersion (σ) of the lensing galaxy has been proposed by Paraficz & Hjorth (2009). They showed that the joint measurement of $\Delta\tau/\sigma^2$ is more effective to constrain cosmological parameters than $\Delta\tau$ or σ^2 separately.

In the GW window, the fantastic sensitivity of the third-generation gravitational-wave interferometric detectors, such as the Einstein Telescope (ET), would significantly improve the detection efficiencies of the GW events. With a large number of detectable events, one may expect that some of these events would be gravitationally lensed by intervening galaxies. The prospects of observing strongly lensed

GWs from merging double compact objects (NS-NS, NS-BH, BH-BH) have been studied in detail (Piórkowska et al. 2013; Biesiada et al. 2014; Ding et al. 2015), and these works predicted that ET would detect about 50–100 strongly lensed GW events per year. This implies that ET will be able to provide a considerable catalog of strongly lensed GWs within a few years of successful operation.

As mentioned above, Liao et al. (2017) proposed that future time delay measurements ($\Delta\tau$) of strongly lensed GW signals accompanied by EM counterparts could be used to obtain robust constraints on cosmological parameters. Since $\Delta\tau/\sigma^2$ is more sensitive to the cosmological parameters than $\Delta\tau$ or σ^2 separately (Paraficz & Hjorth 2009), here we first try to explore the constraint ability of cosmological parameters by the future joint measurements of the precise time delay ($\Delta\tau$) between lensed GW images and the velocity dispersion (σ) of the lensing galaxy in the era of the third-generation gravitational-wave detectors.

The paper is organized as follows. In Section 2, we describe the basics of using strong gravitational lensing systems as standard rulers. In Section 3, we demonstrate that the cosmological parameters can be constrained with great accuracy through the combination $\Delta\tau/\sigma^2$ of the lensed GW-EM system, using Monte Carlo simulations. A brief summary and discussion are given in Section 4.

2 STRONG LENSES AS COSMIC RULERS

A source lensed by a foreground massive galaxy or galaxy cluster appears in multiple images. For a given image i at angle position $\vec{\theta}_i$, with the source position at angle $\vec{\beta}$, the time delay $\Delta\tau_i$ is caused both by the difference in path length between the straight and deflected rays, and the gravitational time dilation of the light ray traveling through the effective gravitational potential $\Psi(\vec{\theta}_i)$ of the lens (Blandford & Narayan 1986):

$$\Delta\tau_i = \frac{1+z_L}{c} \frac{D_{OS}D_{OL}}{D_{LS}} \left[\frac{1}{2}(\vec{\theta}_i - \vec{\beta})^2 - \Psi(\vec{\theta}_i) \right], \quad (1)$$

where z_L is the lens redshift, D_{OS} , D_{OL} , and D_{LS} represent the angular-diameter distances between observer and source, observer and lens, and lens and source, respectively. If the lens potential Ψ and the lens geometry $\vec{\theta}_i - \vec{\beta}$ are known, the time delay measures the ratio $D_{OS}D_{OL}/D_{LS}$, also known as the time-delay distance, which depends on the cosmological parameters. Assuming that the time-delay lensing systems have only two images at $\vec{\theta}_A$ and $\vec{\theta}_B$, and adopting the single isothermal sphere (SIS) model for the gravitational potential of the lens galaxy, the time delay is therefore given by

$$\Delta\tau = \frac{1+z_L}{2c} \frac{D_{OS}D_{OL}}{D_{LS}} (\theta_B^2 - \theta_A^2). \quad (2)$$

The distance ratio that appears in Equation (2) is the time-delay distance, $D_{\Delta\tau} \equiv (1+z_L)D_{OS}D_{OL}/D_{LS}$, which depends primarily on H_0 and has a limited sensitivity to other cosmological parameters, such as Ω_m (more on this below).

Inferring cosmological distances from time-delay lenses also requires accurate models for the mass distribution of the lens galaxy, as well as for any other matter structures along the line-of-sight that may affect the observed time delays between the multiple images (Suyu et al. 2010). A

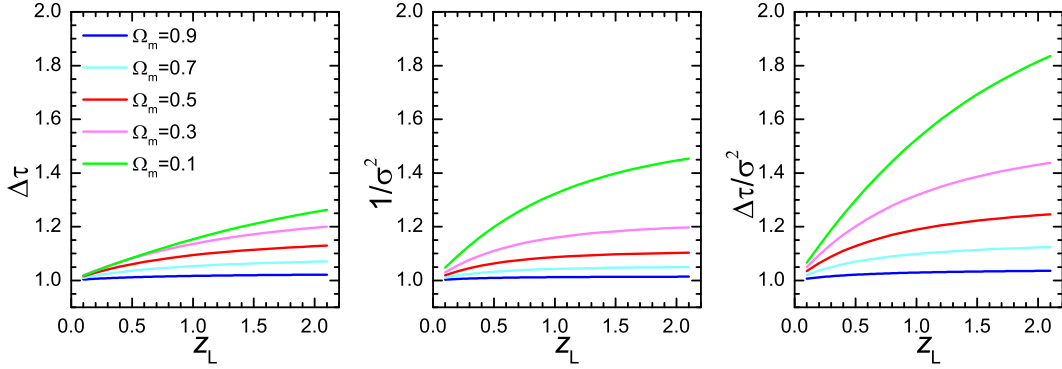


Figure 1. Sensitivity of the three methods ($\Delta\tau$, σ^2 , and $\Delta\tau/\sigma^2$) to the cosmological parameters. The source redshift z_S is fixed to 3. A flat Universe is assumed with five different Ω_m values: 0.1, 0.3, 0.5, 0.7, and 0.9. Each curve is calculated relative to the Einstein-de Sitter Universe.

constant external convergence term κ_{ext} can be absorbed by the lens and source model leaving the fit to the lensed images unchanged, but the true time-delay distance $D_{\Delta\tau}$ altered by a factor of $(1 - \kappa_{\text{ext}})$, i.e.,

$$D_{\Delta\tau} = \frac{D_{\Delta\tau}^{(0)}}{1 - \kappa_{\text{ext}}}, \quad (3)$$

where $D_{\Delta\tau}^{(0)}$ is the time-delay distance inferred from a model not accounting for the effects of weak perturbations along the line-of-sight. To break the “mass-sheet degeneracy” (Falco et al. 1985), one can study the lens environment to constrain κ_{ext} within a few percent based on spectroscopy and multiband wide-field observations of local galaxy groups and line-of-sight structures (e.g., Fassnacht et al. 2006; Momcheva et al. 2006) in combination with ray-tracing through numerical simulations (e.g., Collett et al. 2013; Greene et al. 2013). According to the recent analysis by Collett & Cunningham (2016), the external convergence over an ensemble of lenses usually does not average to zero. Rusu et al. (2017) presented a robust estimate of the external convergence κ_{ext} for the lensed quasar HE 0435-1223, which has a median of 0.004 and a standard deviation of $\delta\kappa_{\text{ext}} = 0.025$. This measured $\delta\kappa_{\text{ext}}$ corresponds to 2.5% uncertainty on $D_{\Delta\tau}$. In sum, the external convergence of each lens is expected to introduce one or two percent extra uncertainty on $D_{\Delta\tau}$ (Collett et al. 2013; Greene et al. 2013; Rusu et al. 2017). Thus, the uncertainty on $D_{\Delta\tau}$ is given by the quadrature sum of the uncertainties on the time delay, external convergence, and image position measurements (Suyu et al. 2017).

The observed velocity dispersion (σ) of the lensing galaxy is the result of the superposition of numerous individual stellar spectra, each of which has been Doppler shifted due to the random stellar motions within the galaxy. Hence, it can be measured by analyzing the integrated spectrum of the galaxy. According to the virial theorem, the velocity dispersion is related to the mass, i.e., $\sigma^2 \propto M_\sigma R$, where M_σ denote the mass enclosed inside the radius R . The mass is determined by the Einstein ring radius θ_E of the lensing system, thus the velocity dispersion in the SIS model can be written as

$$\sigma^2 = \theta_E^2 \frac{c^2}{4\pi} \frac{D_{\text{OS}}}{D_{\text{LS}}}. \quad (4)$$

As shown by Paraficz & Hjorth (2009), two of the angular-diameter distances appearing in Equation (2) could be replaced by the velocity dispersion σ and the Einstein radius $\theta_E = (\theta_A + \theta_B)/2$ ($\Delta\tau$ and $\theta_{A,B}$ are defined to be positive here, with $\theta_B > \theta_A$), i.e.,

$$D_{\text{OL}}(\theta_B - \theta_A) = \frac{c^3}{4\pi} \frac{\Delta\tau}{\sigma^2(1 + z_L)}. \quad (5)$$

In contrast to $D_{\Delta\tau}$, Jee et al. (2015) found that the mass external to the lens along the line-of-sight (external convergence) has no effect on the inferred D_{OL} . The reason is as follows. Assume that there is a lens system which has a time delay of $\Delta\tau$ and a velocity dispersion of σ^2 . We then try to model this system by a lens plus an external convergence, κ_{ext} . The modeled $\Delta\tau$ and σ^2 would be different from the original ones by a factor of $(1 - \kappa_{\text{ext}})$, but the ratio of the two is invariant. Since D_{OL} is proportional to the ratio $\Delta\tau/\sigma^2$, we can determine the same D_{OL} as before, regardless of the existence of the external convergence. Thus, the uncertainty on D_{OL} is given by the quadrature sum of the uncertainties on the time delay, velocity dispersion, and image position measurements (Jee et al. 2015, 2016).

From Equations (2), (4), and (5), we can see that the time-delay $\Delta\tau$ is proportional to $D_{\text{OS}}D_{\text{OL}}/D_{\text{LS}}$, the square of the velocity dispersion σ^2 is proportional to $D_{\text{OS}}/D_{\text{LS}}$, and the ratio $\Delta\tau/\sigma^2$ is dependent only on D_{OL} . That is to say,

$$\Delta\tau \propto \frac{D_{\text{OS}}D_{\text{OL}}}{D_{\text{LS}}}, \quad \sigma^2 \propto \frac{D_{\text{OS}}}{D_{\text{LS}}}, \quad \frac{\Delta\tau}{\sigma^2} \propto D_{\text{OL}}. \quad (6)$$

In Fig. 1, we show the three quantities ($\Delta\tau$, σ^2 , and $\Delta\tau/\sigma^2$) as a function of the lens redshift z_L in the flat Λ CDM model with a fixed source redshift $z_S = 3$ (see also Paraficz & Hjorth 2009). To illustrate the sensitivity of the three functions to Ω_m , we plot them for several cases of a flat Universe with $\Omega_m = 0.1, 0.3, 0.5, 0.7$ and 0.9 , relative to the Einstein-de Sitter Universe ($\Omega_m = 1, \Omega_\Lambda = 0$). One can see from this plot that the $\Delta\tau/\sigma^2$ curves have a wider separation than the $\Delta\tau$ or σ^2 curves to allow an easier discrimination among different cosmological models. This is especially so at high redshifts, thus it is of special significance for the $\Delta\tau/\sigma^2$ method to study high-redshift lenses. Moreover, this method has the advantage of being independent of the source redshift. However, before we put the $\Delta\tau/\sigma^2$

method into practical cosmological uses, we must consider its independence on the other two methods. From their independence tests, [Yuan & Wang \(2015\)](#) found that the methods of $\Delta\tau/\sigma^2$ and σ^2 are not independent; but $\Delta\tau/\sigma^2$ and $\Delta\tau$ are independent, thus we can compare the capability of these two methods to conduct cosmography.

3 TESTING CAPABILITY OF LENSED GW-EM EVENTS TO CONDUCT COSMOGRAPHY

3.1 Monte Carlo simulations

We perform Monte Carlo simulations to test how well the two quantities ($\Delta\tau$ and $\Delta\tau/\sigma^2$) from strongly lensed GW-EM systems can be used to constrain cosmological parameters. To do so, we have to choose a fiducial cosmological model and then simulate a sample of lensed GW-EM systems. Here we adopt the following cosmological parameters of the flat Λ CDM model derived from Planck 2015 data ([Planck Collaboration et al. 2016](#)) in our simulations: $H_0 = 67.8 \text{ km s}^{-1} \text{ Mpc}^{-1}$, $\Omega_m = 0.308$, and $\Omega_\Lambda = 1 - \Omega_m$. Our detailed simulation steps are described as follows:

1. The redshifts of source z_S and lens z_L are randomly generated from the expected redshift probability distribution functions (PDFs) of lensed GW events ([Biesiada et al. 2014](#); [Ding et al. 2015](#)). These redshift PDFs were calculated using the following procedure. Firstly, considering the intrinsic merger rates of the whole class of double compact objects located at different redshifts as calculated by [Dominik et al. \(2013\)](#) and the designed sensitivity of the ET, the yearly detection rate of GW events was estimated. Secondly, the probability that individual GW signal from inspiralling double compact objects could be lensed by early-type galaxy was then calculated. Finally, adding all the double-compact-objects merging systems together, the yearly detection rate of lensed GW events detected by the ET was predicted. This prediction is accompanied by the redshift PDF (see Fig. 2 of [Ding et al. \(2015\)](#)), which enables us to randomly generate the samples of z_S and z_L . Note that short gamma-ray bursts (short GRBs), on-beam GRB afterglow emission, and kilonovae/mergenovae are considered as promising EM counterparts of GW signals. Since $z < 3$ for the current short GRBs, the range of the source redshift z_S for our analysis is from 0 to 3.

2. We simulate the velocity dispersion σ and time delay $\Delta\tau$ separately from the probability distributions of σ and $\Delta\tau$ from the OM10 catalog ([Oguri & Marshall 2010](#)). The OM10 catalog provides mock observations of lensed quasars expected for the baseline survey planned with LSST, based on realistic distributions of quasars and elliptical galaxies as well as the observational condition of this telescope.

3. For the $\Delta\tau$ method, the mock external convergence κ_{ext} is obtained by sampling the PDF of κ_{ext} given by [Rusu et al. \(2017\)](#), we then infer the fiducial value of $\Theta \equiv (\theta_B^2 - \theta_A^2)$ from Equations (2) and (3) using the mock z_S , z_L , κ_{ext} , and $\Delta\tau$. For the $\Delta\tau/\sigma^2$ method, the fiducial value of $\Delta\theta \equiv (\theta_B - \theta_A)$ is inferred from Equation (5) with the mock z_L , σ , and $\Delta\tau$.

4. While the dedicated observations of lensed quasar systems in the EM domain give $\sim 3\%$ uncertainty of the

time delay measurement ([Liao et al. 2015](#)), $\Delta\tau$ obtained from the GW signals are supposed to be very accurate with negligible uncertainty. Therefore, we assign an uncertainty $\delta_{\Delta\tau} = 3\%\Delta\tau$ to the lensed quasar system, and $\delta_{\Delta\tau} \simeq 0$ to the lensed GW-EM system.

5. The current techniques concerning lensed quasar systems in the EM window give a few percent uncertainty of the determination of lens modeling, i.e., $\sim 4\%$ uncertainty on image position measurement Θ (or $\Delta\theta$) and $\sim 10\%$ uncertainty for the observed velocity dispersion σ^2 ([Jee et al. 2015](#)). Note that the bright point spread functions (PSFs) of active galaxy nuclei (AGNs) could induce large systematic errors. In order to extract bright AGN images during the lens modeling procedure, one has to instead use a nearby star's PSF or adopt an iterative PSF modeling process which can accurately recover the PSF for real observations ([Chen et al. 2016](#); [Ding et al. 2017](#); [Wong et al. 2017](#)). However, the systematic errors can not be completely eliminated by these operations. Unlike AGNs, the EM counterparts of GW signals, such as short GRBs and kilonovae, are not always so bright. The lensed images, therefore, might not be affected much by the bright PSFs which are difficult to extract and the exposure time could be longer, making lens modeling so much easier. Based on the current lensing project H0LiCOW¹, [Liao et al. \(2017\)](#) simulated two sets of realistic lensed images with and without the AGN (see [Ding et al. 2017](#) for more details on the simulations). The corresponding exposure time and noise level were set as closely as possible the deep Hubble Space Telescope observations. They found that the effect of bright PSFs can significantly influence the uncertainties of the parameters in the lens model. Therefore, [Liao et al. \(2017\)](#) suggested that the accuracy of lens modeling would be improved to some extent with gravitationally lensed GWs and EM signals. For each lensed GW-EM event, we assign the uncertainties $\delta_\Theta = 2\%\Theta$ (or $\delta_{\Delta\theta} = 2\%\Delta\theta$) and $\delta_{\sigma^2} = 5\%\sigma^2$ to the mock Θ (or $\Delta\theta$) and velocity dispersion σ^2 separately, which are supposed to be the best-case scenarios in the GW era, and are two times smaller than those of the lensed quasar system in the EM domain.

6. It should be underlined that lensed GWs may provide some help on improving lens modeling uncertainty, but do not on the uncertainty of external convergence κ_{ext} . This is because accurately quantifying the mass distribution along the line-of-sight requires wide-field imaging and spectroscopy (see [Treu & Marshall 2016](#) for a recent review), either in lensed quasars or in lensed GWs. [Rusu et al. \(2017\)](#) showed that the uncertainty of κ_{ext} would contribute one or two percent rms error to the value of $D_{\Delta\tau}$ (see also [Collett et al. 2013](#); [Greene et al. 2013](#)), we thus assign an uncertainty $\delta_{\kappa_{\text{ext}}} = 1\%(1 - \kappa_{\text{ext}})$ to the mock κ_{ext} for both the lensed quasar system and the lensed GW-EM system.

7. For every synthetic lens, we add a deviation to the fiducial value of Θ^{fid} (or $\Delta\theta^{\text{fid}}$), i.e., we sample the Θ^{mea} (or $\Delta\theta^{\text{mea}}$) measurement according to the Gaussian distribution $\Theta^{\text{mea}} = \mathcal{N}(\Theta^{\text{fid}}, \sigma_\Theta)$ (or $\Delta\theta^{\text{mea}} = \mathcal{N}(\Delta\theta^{\text{fid}}, \sigma_{\Delta\theta})$).

8. Repeat the above steps to obtain a sample of 50 strong lenses.

¹ <http://h0licow.org>

3.2 Cosmological parameters estimation

For a set of 50 simulated lenses, the likelihood for the cosmological parameters can be determined from the minimum χ^2 statistic:

$$\chi^2(\mathbf{p}) = \sum_i \frac{[\mathcal{D}_i^{\text{obs}} - \mathcal{D}_i^{\text{th}}(\mathbf{p})]^2}{\delta_{\mathcal{D}_i}^2}, \quad (7)$$

where \mathcal{D}^{th} is the theoretical distance calculated from the set of cosmological parameters \mathbf{p} . $\mathcal{D}^{\text{th}} = D_{\text{OS}}D_{\text{OL}}/D_{\text{LS}}$ and $\mathcal{D}^{\text{th}} = D_{\text{OL}}$ correspond to the $\Delta\tau$ method and the $\Delta\tau/\sigma^2$ method, respectively. \mathcal{D}^{obs} is the distance of the simulated observational data sets, and $\delta_{\mathcal{D}}$ is the error of \mathcal{D}^{obs} . With the measured distance \mathcal{D}^{obs} (see Equations (2) and (3)), the propagated error $\delta_{\mathcal{D}_{\Delta\tau}}$ in \mathcal{D}^{obs} using the $\Delta\tau$ method is

$$\delta_{\mathcal{D}_{\Delta\tau}} = \mathcal{D}^{\text{obs}} \left[\left(\frac{\delta_{\Delta\tau}}{\Delta\tau} \right)^2 + \left(\frac{\delta_{\Theta}}{\Theta} \right)^2 + \left(\frac{\delta_{\kappa_{\text{ext}}}}{1 - \kappa_{\text{ext}}} \right)^2 \right]^{1/2}. \quad (8)$$

From Equation (5), the propagated error $\delta_{\mathcal{D}_{\Delta\tau/\sigma^2}}$ in \mathcal{D}^{obs} using the $\Delta\tau/\sigma^2$ method can be written as

$$\delta_{\mathcal{D}_{\Delta\tau/\sigma^2}} = \mathcal{D}^{\text{obs}} \left[\left(\frac{\delta_{\Delta\tau}}{\Delta\tau} \right)^2 + \left(\frac{\delta_{\Delta\theta}}{\Delta\theta} \right)^2 + \left(\frac{\delta_{\sigma^2}}{\sigma^2} \right)^2 \right]^{1/2}, \quad (9)$$

which is dominated by the uncertainty of the velocity dispersion σ^2 (Jee et al. 2015). To ensure the final constraint results are unbiased, we repeat this process 1000 times for each dataset by using different noise seeds.

In Λ CDM, the dark-energy equation of state parameter, w , is exactly -1 . Assuming a flat Universe, $\Omega_{\Lambda} = 1 - \Omega_{\text{m}}$, there are only two free parameters: Ω_{m} and H_0 . We first fix the flat Λ CDM model with $\Omega_{\text{m}} = 0.308$, but keep H_0 as a free parameter. Fig. 2 shows the constraints on H_0 using two different quantities ($\Delta\tau$ and $\Delta\tau/\sigma^2$) from 50 strongly lensed GW-EM systems (solid lines). For comparison, we also plot those constraints obtained from 50 lensed quasars (dashed lines) in the EM domain. One can see that lensed systems observed jointly in GW and EM windows place much more stringent constraints on H_0 than the pure EM lensed systems, independent of what kind of observed quantity ($\Delta\tau$ or $\Delta\tau/\sigma^2$) is adopted. This is mainly due to the fact that the uncertainties of both the time delay and lens modeling in the lensed GW-EM systems are smaller than those of the lensed quasar systems in the EM domain. Using $\Delta\tau$, we find the uncertainty of H_0 from 50 lensed GW-EM systems being $\sim 0.3\%$, compared to $\sim 0.7\%$ from the pure EM lensed systems. Similarly, H_0 is better constrained by 50 lensed GW-EM systems than the pure EM lensed systems with uncertainties of $\sim 0.8\%$ versus $\sim 1.6\%$ using $\Delta\tau/\sigma^2$. Our results are in good agreement with Liao et al. (2017). Not surprisingly, a comparison of Figs. 2(a) with (b) shows that the $\Delta\tau/\sigma^2$ method gives weaker constraints on H_0 than the other method, since the joint observations of time delay and velocity dispersion bring the extra uncertainty from the velocity dispersion (see the comparison between Equations (8) and (9)).

If we relax the priors, and allow both H_0 and Ω_{m} to be free parameters, we obtain the constraints set in the $\Omega_{\text{m}} - H_0$ plane, as illustrated in Fig. 3. In traditional approach using lensed quasar systems observed in the EM domain, one needs a larger sample to increase the significance of the constraints.

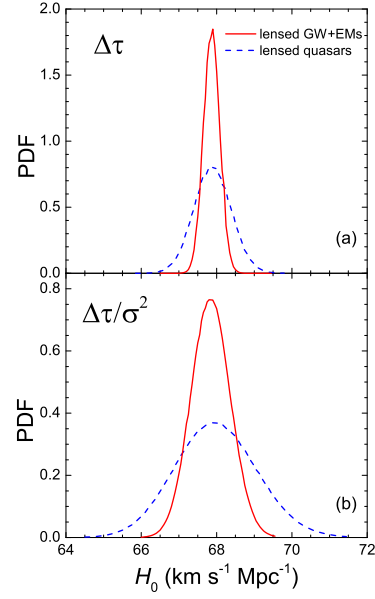


Figure 2. Constraints on the Hubble constant, H_0 , using 50 lensed GW-EM systems (red solid lines) and 50 lensed quasars (blue dashed lines), respectively. (a): Simulations for the $\Delta\tau$ method; (b): same as panel (a), but now for the $\Delta\tau/\sigma^2$ method.

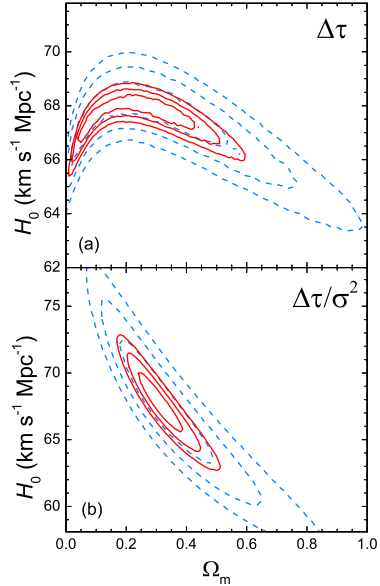


Figure 3. $1\sigma - 3\sigma$ constraint contours of (Ω_{m}, H_0) in the flat Λ CDM model from 50 lensed GW-EM systems (red solid lines) and 50 lensed quasars (blue dashed lines), respectively. (a): Simulations for the $\Delta\tau$ method; (b): same as panel (a), but now for the $\Delta\tau/\sigma^2$ method.

On the contrary, future observations of lensed GWs and their EM counterparts will enable us to achieve precise cosmography from a few dozens of such systems. The constraints on the parameter space from the $\Delta\tau$ method (Fig. 3(a)) give a good constraint on H_0 , but a weak one on Ω_{m} . As expected, the $\Delta\tau/\sigma^2$ method (Fig. 3(b)) gives tighter constraints on Ω_{m} than the other method, i.e., the $\Delta\tau/\sigma^2$ method can improve the discrimination between cosmological models.

For the w CDM model, w is constant but possibly different from -1 . For a flat Universe ($\Omega_k = 0$), there are three free parameters: Ω_{m} , w , and H_0 . Here, we marginalize H_0 in the w CDM model to find the confidence levels in the $\Omega_{\text{m}} - w$

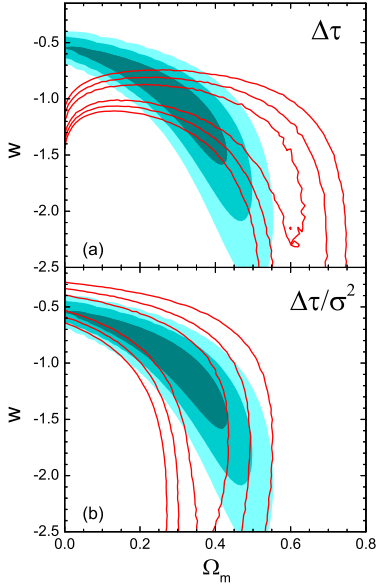


Figure 4. Constraint results for the w CDM model using 50 lensed GW-EM systems (red solid lines), compared with those associated with the 580 Union2.1 SNe Ia data (shaded contours). (a): Simulations for the $\Delta\tau$ method; (b): same as panel (a), but now for the $\Delta\tau/\sigma^2$ method.

plane. We demonstrate that lensed GW-EM systems can be a viable way to constrain dark energy equation of state. To gauge the impact of these constraints more clearly, we show in Fig. 4 the confidence regions (red solid lines) for Ω_m and w using 50 simulated strongly lensed GW-EM systems, and compare these to the constraint contours for the 580 Union2.1 SNe Ia data (Suzuki et al. 2012) (represented by the shaded contours in Fig. 4). It is straightforward to see how effectively the lensed GW-EM systems could be used as a cosmological probe. With a sample size of several tens, the contour size of lensed GW-EM systems is already comparable to that of 580 SNe Ia data. Furthermore, we note that the constraints obtained from the $\Delta\tau$ method (Fig. 4(a)) and the $\Delta\tau/\sigma^2$ method (Fig. 4(b)) are intersecting, much more severe constraints can be achieved when combining these two methods.

4 SUMMARY AND DISCUSSION

Although the constraints on cosmological parameters have reached high precision, all of the constraints so far have relied on EM observations alone. New multi-messenger signals exploiting different emission channels are essential for probing cosmology to a higher accuracy level. Recently, Liao et al. (2017) proposed that future time delay measurements of strongly lensed GW signals and their EM counterparts have great potential to infer cosmological parameters. Compared to the traditional approach using strongly lensed quasar systems observed in the EM domain, the approach with lensed systems observed in both GW and EM windows has two advantages in constraining cosmological parameters. Firstly, the time delays ($\Delta\tau$) between lensed images inferred from the GW signals would reach an extremely high accuracy (~ 0.1 s) from the detection pipeline, and such accurate

measurements of $\Delta\tau$ would play an important role in boosting the development of precision cosmology. Secondly, with gravitationally lensed GWs and EM signals, the accuracy of lens modeling could be improved to some extent, leading to better constraints on cosmological parameters.

In the EM window, Paraficz & Hjorth (2009) suggested that the joint observations of the time delay ($\Delta\tau$) between lensed quasar images and the velocity dispersion (σ) of the lensing galaxy are more effective to constrain cosmological parameters than $\Delta\tau$ or σ^2 separately. In this work, we apply the $\Delta\tau/\sigma^2$ method, for the first time, to the strongly lensed systems observed in both GW and EM windows. We prove that both $\Delta\tau$ and $\Delta\tau/\sigma^2$ from strongly lensed GW-EM systems can serve as powerful cosmic rulers. From the comparison of the two different methods, we confirm that the $\Delta\tau/\sigma^2$ method can provide tighter constraints on Ω_m than the $\Delta\tau$ method, i.e., using $\Delta\tau/\sigma^2$ can make us easier to differentiate different cosmological models. Furthermore, we show that with a moderate sample size of several tens, one may reach a constraint on the dark energy equation of state w comparable to the 580 Union2.1 SNe Ia sample. Combining the $\Delta\tau$ and $\Delta\tau/\sigma^2$ methods, one may achieve unprecedented accuracy in constraining w .

The recent Advanced LIGO observations of binary black hole mergers GW150914 (Abbott et al. 2016a), GW151226 (Abbott et al. 2016b), and GW170104 (Abbott et al. 2017) have initiated the era of GW astronomy. Thanks to the great high sensitivity, the planned third-generation gravitational-wave detectors, such as the ET, could observe the strongly lensed GWs. If in the future gravitationally lensed GWs and their EM counterparts are detected simultaneously, the prospects for the study of cosmology with such lensing systems, as discussed in this work, will be very promising.

ACKNOWLEDGEMENTS

We thank Kai Liao for his kind assistance. This work is partially supported by the National Basic Research Program (“973” Program) of China (Grant No. 2014CB845800), the National Natural Science Foundation of China (Grant Nos. 11673068, 11603076, 11433009, and 11373068), the Youth Innovation Promotion Association (2011231 and 2017366), the Key Research Program of Frontier Sciences (QYZDB-SW-SYS005), the Strategic Priority Research Program “Multi-waveband gravitational wave Universe” (Grant No. XDB23000000) of the Chinese Academy of Sciences, the Natural Science Foundation of Jiangsu Province (Grant No. BK20161096), and the Guangxi Key Laboratory for Relativistic Astrophysics.

REFERENCES

- Abbott B. P., et al., 2016a, *Physical Review Letters*, **116**, 061102
- Abbott B. P., et al., 2016b, *Physical Review Letters*, **116**, 241103
- Abbott B. P., et al., 2017, *Physical Review Letters*, **118**, 221101
- Anderson L., et al., 2012, *MNRAS*, **427**, 3435
- Baker T., Trodden M., 2017, *Phys. Rev. D*, **95**, 063512
- Beutler F., et al., 2011, *MNRAS*, **416**, 3017
- Biesiada M., Piórkowska A., Malec B., 2010, *MNRAS*, **406**, 1055
- Biesiada M., Ding X., Piórkowska A., Zhu Z.-H., 2014, *J. Cosmology Astropart. Phys.*, **10**, 080

- Blandford R., Narayan R., 1986, *ApJ*, **310**, 568
- Bonvin V., et al., 2017, *MNRAS*, **465**, 4914
- Cai R.-G., Yang T., 2017, *Phys. Rev. D*, **95**, 044024
- Cao S., Pan Y., Biesiada M., Godlowski W., Zhu Z.-H., 2012, *J. Cosmology Astropart. Phys.*, **3**, 016
- Chen G. C.-F., et al., 2016, *MNRAS*, **462**, 3457
- Coe D., Moustakas L. A., 2009, *ApJ*, **706**, 45
- Collett T. E., Bacon D., 2017, *Physical Review Letters*, **118**, 091101
- Collett T. E., Cunningham S. D., 2016, *MNRAS*, **462**, 3255
- Collett T. E., et al., 2013, *MNRAS*, **432**, 679
- Del Pozzo W., Li T. G. F., Messenger C., 2017, *Phys. Rev. D*, **95**, 043502
- Ding X., Biesiada M., Zhu Z.-H., 2015, *J. Cosmology Astropart. Phys.*, **12**, 006
- Ding X., et al., 2017, *MNRAS*, **465**, 4634
- Dobke B. M., King L. J., Fassnacht C. D., Auger M. W., 2009, *MNRAS*, **397**, 311
- Dobler G., Fassnacht C. D., Treu T., Marshall P., Liao K., Hojjati A., Linder E., Rumbaugh N., 2015, *ApJ*, **799**, 168
- Dominik M., Belczynski K., Fryer C., Holz D. E., Berti E., Bulik T., Mandel I., O’Shaughnessy R., 2013, *ApJ*, **779**, 72
- Falco E. E., Gorenstein M. V., Shapiro I. I., 1985, *ApJ*, **289**, L1
- Fan X.-L., Liao K., Biesiada M., Piórkowska-Kurpas A., Zhu Z.-H., 2017, *Physical Review Letters*, **118**, 091102
- Fassnacht C. D., Gal R. R., Lubin L. M., McKean J. P., Squires G. K., Readhead A. C. S., 2006, *ApJ*, **642**, 30
- Greene Z. S., et al., 2013, *ApJ*, **768**, 39
- Grillo C., Lombardi M., Bertin G., 2008, *A&A*, **477**, 397
- Hinshaw G., et al., 2013, *ApJS*, **208**, 19
- Holz D. E., Hughes S. A., 2005, *ApJ*, **629**, 15
- Jee I., Komatsu E., Suyu S. H., 2015, *J. Cosmology Astropart. Phys.*, **11**, 033
- Jee I., Komatsu E., Suyu S. H., Huterer D., 2016, *J. Cosmology Astropart. Phys.*, **4**, 031
- Liao K., et al., 2015, *ApJ*, **800**, 11
- Liao K., Fan X.-L., Ding X.-H., Biesiada M., Zhu Z.-H., 2017, preprint, ([arXiv:1703.04151](https://arxiv.org/abs/1703.04151))
- Melia F., Wei J.-J., Wu X.-F., 2015, *AJ*, **149**, 2
- Momcheva I., Williams K., Keeton C., Zabludoff A., 2006, *ApJ*, **641**, 169
- Oguri M., Marshall P. J., 2010, *MNRAS*, **405**, 2579
- Paraficz D., Hjorth J., 2009, *A&A*, **507**, L49
- Paraficz D., Hjorth J., 2010, *ApJ*, **712**, 1378
- Perlmutter S., et al., 1998, *Nature*, **391**, 51
- Piórkowska A., Biesiada M., Zhu Z.-H., 2013, *J. Cosmology Astropart. Phys.*, **10**, 022
- Planck Collaboration et al., 2016, *A&A*, **594**, A13
- Refsdal S., 1964, *MNRAS*, **128**, 307
- Riess A. G., et al., 1998, *AJ*, **116**, 1009
- Rusu C. E., et al., 2017, *MNRAS*, **467**, 4220
- Schmidt B. P., et al., 1998, *ApJ*, **507**, 46
- Schutz B. F., 1986, *Nature*, **323**, 310
- Sereno M., Paraficz D., 2014, *MNRAS*, **437**, 600
- Suyu S. H., Marshall P. J., Auger M. W., Hilbert S., Blandford R. D., Koopmans L. V. E., Fassnacht C. D., Treu T., 2010, *ApJ*, **711**, 201
- Suyu S. H., et al., 2013, *ApJ*, **766**, 70
- Suyu S. H., et al., 2017, *MNRAS*, **468**, 2590
- Suzuki N., et al., 2012, *ApJ*, **746**, 85
- Treu T., 2010, *ARA&A*, **48**, 87
- Treu T., Marshall P. J., 2016, *A&ARv*, **24**, 11
- Wei J.-J., Wu X.-F., Melia F., 2014, *ApJ*, **788**, 190
- Wong K. C., et al., 2017, *MNRAS*, **465**, 4895
- Yuan C. C., Wang F. Y., 2015, *MNRAS*, **452**, 2423
- Zhu Z.-H., 2000, *International Journal of Modern Physics D*, **9**, 591
- Zhu Z.-H., Sereno M., 2008, *A&A*, **487**, 831

This paper has been typeset from a $\text{\TeX}/\text{\LaTeX}$ file prepared by the author.